PHYSICAL REVIEW B VOLUME 16, NUMBER 11 1 DECEMBER 1977

Optical measurement of the hyperfine splitting of the $^1D_2$ metastable state of Pr^{3+} in LaF_3 by enhanced and saturated absorption spectroscopy

L. E. Erickson
National Research Council, Ottawa, Canada K1A 0R8
(Received 29 June 1977)

The sizable ground-state nuclear polarization which accompanies the optical pumping of the $^3H_4$-$^1D_2$ (16 872-cm^{-1}) σ transition of Pr^{3+} in LaF_3 was utilized to observe enhanced and saturated absorptions within the inhomogeneously broadened spectral line. The observed hyperfine splittings of the lowest $^1D_2$ state are 3.7 and 4.7 MHz at 2.0°K. These splittings were fitted by a spin Hamiltonian $\mathcal{H} = D[I_z^2 - I(I+1)/3] + (E/2)(I_+^2 + I_-^2)$, where $D = -1.10 \pm 0.05$ and $E = -0.48 \pm 0.05$ MHz. The observed linewidths (including the exciting laser linewidth) were 0.8 MHz. The deconvoluted optical transition linewidths (full widths at half-maximum) are 0.20 ± 0.05 MHz.

INTRODUCTION

Narrow linewidth tunable laser sources have made possible measurement of the hyperfine structure of the ground state of ions in dielectric solids[1,2] where inhomogeneous broadening of the spectral lines inhibits the use of normal spectroscopic techniques.[3] Hutchison and co-workers[4] have observed the hyperfine structure of the ground and excited states of rare-earth and actinide ions in lanthanum trichloride ($LaCl_3$) using rf optical techniques in large magnetic fields. In this paper are reported the first measurements of the hyperfine splittings of the excited metastable $^1D_2$ (16 872-cm^{-1}) state of trivalent praseodymium dilute in single-crystal lanthanum trifluoride. This result is important because of the current interest in time domain (free-induction decay,[5] photon echoes[6]) and frequency domain (fluorescence line narrowing[7]) experiments in the $^1D_2 \leftrightarrow {}^3H_4$ transition.

The observations were made using an optical hole-burning and optical pumping technique with which both *enhanced*-absorption and *saturated*-absorption optical-spectral-line frequencies and linewidths were measured. While Hutchison *et al*[4] observed enhanced optical absorption in the presence of both an electron-paramagnetic-resonance microwave field and a static external magnetic field, and in Ref. 1 I have reported enhanced optical absorption in the presence of magnetic dipole transitions between ground-state hyperfine levels in zero external magnetic field, this paper is the first reported observation of *enhanced* absorption (antiholes) in the presence of purely optical excitation in solids.

The narrowest spectral components of the lines of rare-earth ions dilute in dielectric solids are those which result from transitions between the lowest states of two crystal-field-split levels. These components are inhomogeneously broadened by the variation in the crystalline electric field in the imperfect crystal. This broadening is about 4 GHz for a LaF_3:0.05-at.%-Pr^{3+} single crystal. In the LaF_3:Pr^{3+} system the crystalline electric field site symmetry is low enough (C_2) to remove all electronic degeneracy. All first-order magnetic hyperfine interactions disappear in the absence of an external magnetic field. The nuclear-quadrupole interaction and the second-order magnetic-dipole hyperfine interactions produce three doubly degenerate hyperfine states for each nondegenerate electronic state. This hyperfine splitting, of order 10 MHz for the ground state,[1] is dominated by the second-order magnetic hyperfine interaction. The $^1D_2$ excited-state splitting should be slightly smaller because the smaller angular momentum $J = 2$ more than offsets the closer spacing of nearest electronic energy levels and the hyperfine interaction constant A_J is smaller for the $^1D_2$ state than for the $^3H_4$ ground state.

EXPERIMENT

The experiment devised to measure the small excited state splitting in the presence of the large inhomogeneously broadened background is shown schematically in Fig. 1. Consider the excitation of an ensemble of ions whose 2—5 transition frequency is in resonance with a monochromatic source of light. The upper state may decay radiatively to any of the ground states.[8] Only ions in state 2 are optically pumped. After a large number of excitation cycles the ground-state population ratios are no longer described by a Boltzmann distribution. The population of level 2 is depleted because the 1, 2 and 3, 2 nuclear spin lattice

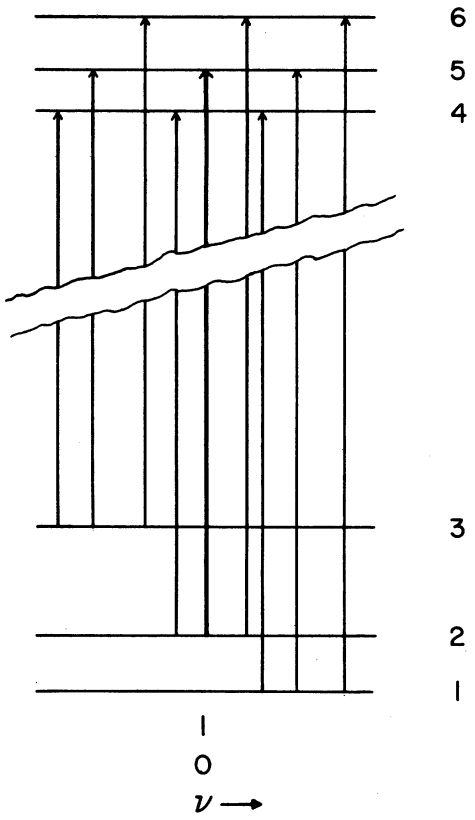

FIG. 1. Energy-level diagram showing the optical transitions between two hyperfine-split electronic states in zero external static magnetic field. The levels are labeled in numerical order to facilitate the discussion. The diagram is about 33 MHz wide for praseodymium in lanthanum trifluoride. The zero on the horizontal axis is measured from the frequency of the saturating laser.

relaxation times are long compared to the excitation rates. A weak probe beam is used to observe absorptions from levels 1, 2 or 3 to levels 4, 5 or 6. For transitions from states 1 and 3 to states 4, 5 and 6 of the pumped ions, the absorption should be larger than for the unpumped ions because the population of levels 1 and 3 are larger for the pumped ions. For transitions from level 2 to levels 4, 5 and 6, the absorptions should be smaller than for the unpumped ions. In the background of the inhomogeneous profile of unpumped ions we should see *enhanced* absorptions (antiholes) from the former and *saturated* absorptions (holes) from the latter. The linewidths should be a convolution of the exciting laser linewidth, the probe laser linewidth and twice the homogeneous width of the optical transition. The homogeneous width of the optical transition appears twice because the hole burnt in the ground-state

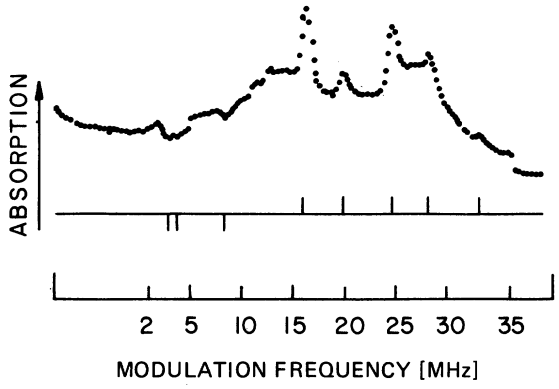

FIG. 2. Saturated and enhanced absorption spectrum of $LaF_3:Pr^{3+}$ at 2°K. The modulation frequency is the difference in optical frequencies between the saturating laser and the probe laser. The absorption of probe light is proportional to the fluorescence amplitude (vertical axis). The sweep begins at 1.4 MHz.

population cannot be narrower than the homogeneous linewidth of the optical transition which produces it. The resulting hole is probed by a similar or the same optical transition which adds the homogeneous width of the probe transition to the observed width. Eight other ion types corresponding to the remaining transitions which connect all upper states with all lower states must be considered in order to obtain the composite spectrum. The transition probabilities of the pump transition vary widely for the nine different ion types so all will not contribute equally to the observed enhanced and saturated optical absorptions.

A single crystal of Pr^{3+} (0.05 at.%) dilute in LaF_3,

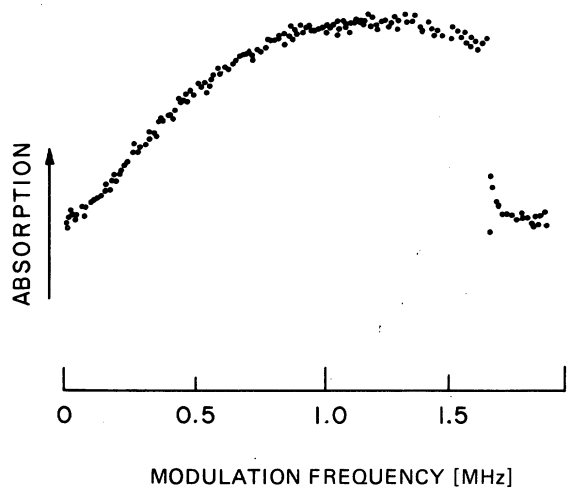

FIG. 3. Saturated absorption spectrum near zero optical frequency difference between saturation and probe beams. The observed half-width at half-maximum amplitude is 0.42±0.02 MHz.

immersed in liquid helium at 2.0 °K, was illuminated by a 1-mW beam (2-mm diam.) from a single-frequency stabilized cw dye laser to excite the $^3H_4(0\text{-cm}^{-1}) \rightarrow {}^1D_2(16\,872\text{-cm}^{-1})$ σ transition.[7] Optical absorption was monitored by observation of fluorescence from the crystal in the $^1D_2(16\,872\text{-cm}^{-1}) \rightarrow {}^3H_4(197\text{-cm}^{-1})$ π transition. A weak probe beam was generated by amplitude modulation of the laser beam. Approximately 1% of the laser power was in the sidebands. The probe beam frequency was swept from 1.4 to 35 MHz in about 70 sec. An automatic bias correction was required to correct for thermal drift of the electro-optical modulator. A typical scan is shown in Fig. 2. The predominant features are as follows: three enhanced absorptions are noted 16.7, 20.4, and 25.2 MHz, weaker enhanced absorptions are noted at 21.4, and 28.8 MHz, and saturated absorptions are observed at 3.7, 4.7 and 8.8 MHz. The observed linewidths [full widths at half-maximum (FWHM)] vary from 0.80 to 1.0 MHz at 2 °K. The amplitudes of the enhanced absorptions are proportional to the sideband power. The large broad amplitude fluctuations are due to sideband amplitude changes versus modulation frequency and are not related to the LaF_3: Pr^{3+} crystal. The saturated absorption at zero frequency was scanned from 30 KHz to 1.5 MHz. A typical result is shown in Fig. 3. The observed half-width at half-maximum of 0.42 ± 0.02 MHz at 2 °K increases to 0.75 ± 0.04 MHz at 4.5 °K. This observed increase in the FWHM of 0.66 MHz is less than the 1.1-MHz (convoluted) FWHM increase expected from single-phonon processes.[6] The shape of this absorption line was analyzed in an attempt to determine the nature of the broadening mechanisms. The accuracy of the measurement was insufficient to determine the line shape other than to say it was

TABLE I. Spectroscopy of LaF_3:Pr^{3+} at 2 °K.

Best-fit frequency	Observed frequency: No rf (MHz)	8.47 MHz rf (MHz)	16.70 MHz rf (MHz)	Calculated intensity $D=-1.10$	Calculated intensity $D=+1.28$ MHz	Line width[a] 2 °K
Enhanced absorption						
33.602		33.7	33.7	0.754	0.000	
29.877				0.031	0.000	
28.895	28.77 ± 0.08	28.8	28.8	0.142	0.001	1.00 ± 0.05
25.170				0.067	0.020	
25.132	25.17 ± 0.03	25.2	25.2	0.165	0.000	0.96 ± 0.05
21.445				0.002	0.005	
21.407		21.4		0.007	0.000	
20.463		20.4		0.003	0.090	
20.425	20.38 ± 0.03		20.4	0.761	0.008	0.80 ± 0.05
16.902				0.011	0.001	
16.738	16.67 ± 0.04		16.7	0.001	0.885	0.94 ± 0.05
16.700		16.6		0.049	0.007	
13.177		13.0		0.650	0.011	
12.975			12.2	0.001	0.001	
12.196		12.0		0.002	0.009	
11.993				0.018	0.892	
8.470		8.3	8.40	0.141	0.167	
8.268				0.000	0.093	
4.745				0.038	0.811	
3.763			3.7	0.026	0.000	
0.038				0.008	0.001	
Saturated absorption						
8.432	8.68[b]					
4.707	4.66 ± 0.05		4.7			0.85 ± 0.05
3.725	3.72 ± 0.08					0.96 ± 0.05
0	0					0.84 ± 0.04

[a] The linewidths at 4.5 °K of the 16.7-MHz transition is 1.7 MHz and the 25.2-MHz transition is 1.8 MHz. This is the total linewidth observed. The deconvoluted homogeneous linewidths are 0.65 ± 0.05 and 0.70 ± 0.05 MHz, respectively.

[b] The line shape is distorted by a sharp cutoff on the low-frequency side.

between a Lorentz and Gaussian line shape. The 2 °K saturated absorption width changed less than 10% for a 100-fold decrease in laser saturating power.

The observed frequencies at 2 °K for the saturated and enhanced absorptions are given in column 2 of Table I. Since the saturated absorptions result from a common lower state, the upper-state splittings are approximately 3.7 and 4.7 MHz. The best fit of three excited states and three ground states to all of the experimental data is given in column 1 of Table I. Most of the enhanced absorptions 16.7 MHz and higher are observed. All of the saturated absorptions are observed. The absence of the enhanced absorptions at frequencies less than 16 MHz may be related to the smaller ground-state nuclear-quadrupole-resonance signal observed for the low-frequency transition.[1] This was due to population differences between quadrupole levels being substantially smaller for the low-frequency transition than for the higher-frequency transition. If the low-frequency enhanced absorptions are not observable because of these small population differences, then an rf magnetic field at the ground-state nuclear-quadrupole-resonance (NQR) frequencies should produce the missing enhanced absorptions. An rf magnetic field of ~0.4 Oe was applied to the sample at the two ground-state frequencies. Typical results for the two separate (ground-state) resonant frequencies are shown in Figs. 4 and 5. All of the enhanced absorptions with significant transition probabilities predicted in Table I and not previously observed are present in Figs. 4 and 5. The observed frequencies are listed in columns 3 and 4 of Table I. A confirmation of this assignment was sought by attempting to induce observable magnetic-dipole transitions in the excited state with an rf magnetic field of

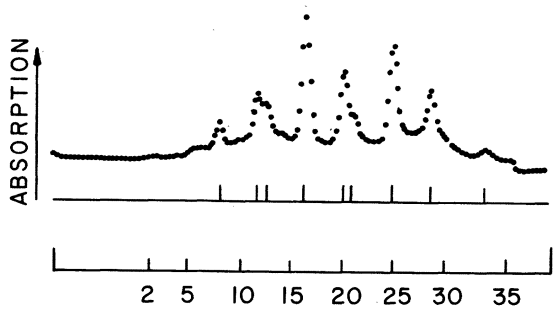

FIG. 4. Enhanced and saturated absorption spectrum of $LaF_3:Pr^{3+}$ at 2°K in the presence of an rf magnetic field at the ground-state NQR frequency. The rf magnetic field frequency is 8.47 MHz.

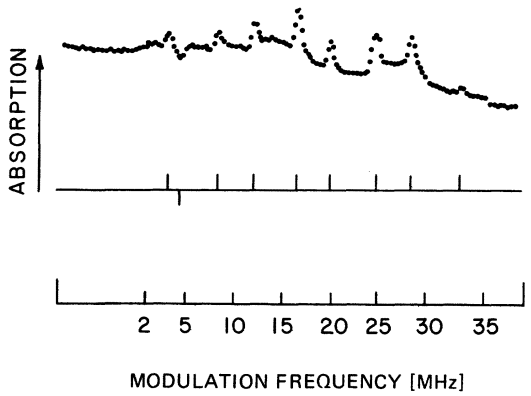

FIG. 5. rf magnetic field frequency is 16.70 MHz. Otherwise as in Fig. 4.

0.7 G of frequency in the neighborhood of the best-fit upper frequencies. No change in fluorescence was observed. The upper-state lifetime of 0.5 msec is too short to permit detection of magnetic resonance with our signal-to-noise ratio of 100 for the ground state where the limiting lifetime is several seconds.

A calculation of the optical-transition probabilities for the nine transitions was necessary in order to confirm the model dynamics and the observed structure and line assignment. The upper-state energy level separations can be fitted by a spin Hamiltonian[9]

$$\mathcal{H}=D[I_z^2-\tfrac{1}{3}I(I+1)]+\tfrac{1}{2}E(I_+^2+I_-^2)\,, \tag{1}$$

where

$$D=A_J[\tfrac{1}{2}(\Lambda_{xx}+\Lambda_{yy})-\Lambda_{zz}]+P\,, \tag{2}$$

$$E=A_J[\tfrac{1}{2}(\Lambda_{yy}-\Lambda_{xx})]+\tfrac{1}{3}\eta P\,, \tag{3}$$

$$\Lambda_{ii}=\sum_{n\neq 0}\frac{A_J|\langle 0|J_i|n\rangle|^2}{E_n-E_0}\,, \tag{4}$$

where A_J is the hyperfine interaction constant, E_n, $|n\rangle$ are the energy and the wave function of the nth crystal-field level, and $|0\rangle$ represents the level being considered. P, η are the normal nuclear-electric-quadrupole interaction constants. This Hamiltonian fits the data for two sets of parameters

$$D=1.27\pm0.050\ \text{MHz},\quad E=0.308\pm0.03\ \text{MHz},$$

or

$$D=-1.100\pm0.050\ \text{MHz},\quad E=-0.483\pm0.05\ \text{MHz}.$$

The signs are relative to the ground-state results.[1] A calculation of the optical transition probability provides one means of distinguishing between the two parameter sets. The electronic part of the transition probability is the same for all

nuclear substate pairs in the optical transition. The relative intensities are determined by the nuclear overlap integrals between the upper and lower states because the optical transitions are electric dipole

$$I_{ij} \sim |\langle E_j | G_i \rangle|^2, \quad i = 1,3, \quad j = 4,6,$$

where I_{ij} is proportional to the intensity of the optical transition connecting states i,j. The intensities for the two parameter sets are given in Table II.

The saturated and enhanced absorption intensities are functions of both the population differences between the three ground hyperfine states and the transition intensities from Table II. The populations of the hyperfine states for each ion type are determined by the intensity of the pump transition, the intensity of the pump, the branching ratios from the upper state to the three lower states and the nuclear-spin-lattice relaxation times between the ground hyperfine states. Because of the absence of measurements of the two ground-state relaxation times, a calculation of a dynamic model was not attempted. However a simple product of the intensities of the two transitions involved give us a first approximation of the saturated and enhanced absorption intensities. These are shown in column 5 of Table I for the two sets of parameters which fit the experimental data. As can be seen from the table, the observed enhanced and saturated absorption intensities are fitted by the calculated intensities more closely with the last choice of parameters.

A calculation of the parameters D and E was made to attempt to distinguish between the two sets of parameters on a physical basis. Unfortunately, a set of crystal-field parameters which give the correct experimental energy levels and symmetries is not available. An examination of the $^1D_2$ energy level symmetries shows that Λ_{xx} and Λ_{yy} will be larger than Λ_{zz} because of the close proximity of an energy level of $|J_z|_{max} = 1$ to the $|J_z|_{max} = 2$ lowest level (23 cm^{-1}). The closest energy level $|J_z|_{max} = 2$ lies some 314 cm^{-1} (measured) above the lowest $^1D_2$ energy level. Equation (2) then gives us the sign of D as $+ve$. Since the measured sign is relative to that of the ground state, and the ground-state sign of D is negative from similar considerations, [10] the parameter set.

$$D = -1.10 \pm 0.05 \quad \text{and} \quad |E| = 0.48 \pm 0.05$$

should be chosen on these physical considerations. A calculation of D and E was made using wavefunctions of Matthies and Welsch[11] for the $LaF_3:Pr^{3+}$. The second-order contributions to the hyperfine structure are $D = +0.20$ MHz and $E = -0.46$ MHz. Although the magnitudes of these calculated values are not very accurate, the signs are consistent with the simple physical model and together with the intensity evidence, they give considerable confidence in the choice of a parameter set for the spin Hamiltonian.

The linewidths of the enhanced absorptions and the saturated absorptions are the result of lifetime limiting processes such as relaxation of upper levels by phonon and photon processes and to magnetic interactions between the praseodymium ions (and nuclei) and their neighboring nuclear dipoles fluorine and lanthanum. At 2 °K the radiative width for the $^1D_2$(16 872-cm^{-1}) $\rightarrow$ $^3H_4$(0-cm^{-1}) transition is 600 Hz, [12] the one-phonon width is 800 Hz,[7] and the magnetic width is approximately 200 kHz for the strongest

TABLE II. Transition intensities for the optical transitions connecting the $^3H_4$ ground state to the $^1D_2$ (16 872-cm^{-1}) state. The states are labeled in numerical order of increasing energy as in Fig. 1.

	$D = -1.100$ MHz	$E = -0.483$ MHz	
	4	5	6
1	0.0465	0.1509	0.8027
2	0.0142	0.8103	0.1755
3	0.9394	0.0388	0.0218
	$D = +1.276$ MHz	$E = 0.308$ MHz	
	4	5	6
1	0.8971	0.0911	0.0118
2	0.0945	0.9039	0.0016
3	0.0083	0.0051	0.9866

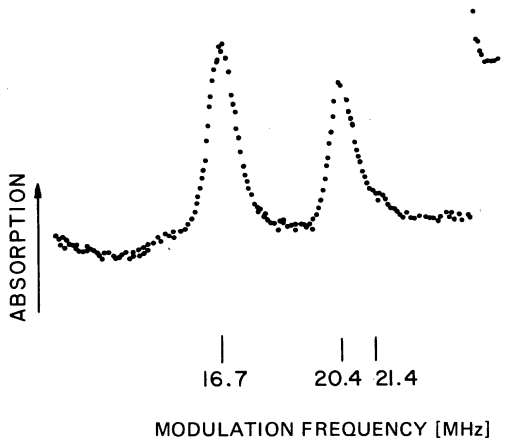

FIG. 6. Enhanced absorption spectrum of the 16.7- and 20.4-MHz transitions. The linewidths (FWHM) on this run are 1.0 ± 0.05 and 0.89 ± 0.05 MHz, respectively.

transitions.[13] The 16.7- and 20.4-MHz enhanced-absorption transitions are shown in Fig. 6. The measure linewidths are 1.0 ± 0.05 and 0.89 ± 0.05 MHz FWHM, respectively, for this run. All of the measurements made on these two transitions show a difference in linewidth of 100 $\pm$ 20 kHz.

The homogeneous linewidth may be estimated from the measured linewidth.[14] The total observed linewidth will be $\Delta_1 + L$ in hole preparation and $\Delta_2 + L$ in observation where Δ_1 is the linewidth (FWHM) of the saturating transition, Δ_2 is the linewidth of the probe transition, and L is the laser jitter linewidth. The laser jitter linewidth of 0.2-MHz FWHM, was estimated from the correction voltage in the laser-frequency stabilizer. The jitter frequency spectrum appears to be noise of frequencies greater than 1 kHz. The laser-reference cavity for the stabilizer had a 40-kHz peak-to-peak jitter at frequencies less than 100 Hz. The narrowest observed linewidths of 800 kHz deconvolute to a homogeneous width of 200 ± 50 kHz. The large uncertainty is due to the accuracy of determination of the laser linewidth.

This experimentally determined optical linewidth is substantially less than the free-induction-decay measurement of 830-kHz FWHM by Genack *et al.*[5] The predicted optical linewidths[1] due to nuclear-dipole—nuclear-dipole interactions between neighboring fluorine and lanthanum nuclei and the praseodymium nuclei 74 to 198 kHz are consistent with this measured value of 200 ± 50 kHz. I therefore conclude that the optical linewidths can be explained by a nuclear-dipole superhyperfine interaction at 2 °K. This conclusion should be confirmed by a detailed study of the different optical transitions whose widths will depend on the changes in the projections of the nuclear moments along the Z axis for the optical transitions.

This measurement of the $^1D_2$ hyperfine splitting was made possible by the substantial nuclear polarization which accompanies narrowband excitation of the $^3H_4(0\text{-cm}^{-1}) \rightarrow {}^1D_2(16\,872\text{-cm}^{-1})$ transition in $LaF_3:Pr^{3+}$. It is applicable to any system in which similar optical pumping occurs. The method allows detailed study of the optical transitions between hyperfine states which make possible a means for determining the nature of the broadening mechanisms in solids at low temperatures.

ACKNOWLEDGMENTS

I wish to thank A. Szabo for many stimulating discussions and E. Dimock for technical assistance.

[1] L. E. Erickson, Opt. Commun. 21, 147 (1977).
[2] C. Delsart, N. Pelletier-Allard, and R. Pelletier, Opt. Commun. 16, 114 (1976).
[3] G. H. Dieke and B. Pandley, J. Chem. Phys. 41, 1952 (1964).
[4] C. A. Hutchison, Jr. and E. D. Lui, J. Lumin. 12,13, 665 (1976).
[5] A. Z. Genack, R. M. MacFarlane, and R. G. Brewer, Phys. Rev. Lett. 37, 1078 (1976).
[6] Y. C. Chen and S. R. Hartmann, Phys. Lett. A58, 201 (1976).
[7] L. E. Erickson, Opt. Commun. 15, 246 (1975).
[8] The largest intensity transition connects states 2 and 5. However, weak nuclear state mixing due to nonaxial hyperfine interaction leads to nonzero probability for 5-1 and 5-3 radiative transitions.
[9] M. A. Teplov, Sov. Phys.-JETP 26, 872 (1968).
[10] The $^3H_4$ crystal-field states at 0, 57, and 78 cm^{-1} all have $|J_z|_{max} = 4$. The crystal-field level at 138 cm^{-1} has $|J_z|_{max} = 3$. Therefore the $\Lambda_{zz} >> \Lambda_{xx}, \Lambda_{yy}$ and D is negative for the $^3H_4$ (0-cm^{-1}) crystal-field state. This experiment cannot determine the absolute sign of D.
[11] S. Matthies and D. Welsch (private communication); see also, Phys. Status Solidi B 68, 125 (1975).
[12] M. J. Weber, J. Chem. Phys. 48, 4774 (1968).
[13] The magnetic width is inferred from the measurements of Ref. 1. The induced magnetic moment of the Pr^{3+} ion in the lowest $^1D_2$ state is assumed to be zero in the z direction since the nearest state contributing to Λ_{zz} is 314 cm^{-1} above. The x and y components of the induced moment, if included, should increase this estimate slightly.
[14] The exact form of the deconvolution is not known. The estimate of the homogeneous linewidth given here is exact if the homogeneous line and the dye-laser spectral density have a Lorentzian form.